

SELECTION OF THE OPTIMUM LANDSAT THEMATIC MAPPER BANDS FOR AUTOMATIC LINEAMENTS EXTRACTION, WADI NATASH AREA, SOUTH EASTERN DESERT, EGYPT

Ahmed A. Madani

Assistant Professor - Cairo University, Faculty of Science,
Geology Department, Giza, Egypt.

Tel: (002)-02-5547713 (Res.) Fax: (002)-02-5727556

E-mail: aamadani18@hotmail.com

KEY WORDS: Automatic Lineament Extraction, Landsat TM Bands, GeoAnalyst PCI EASI/PACE Software

ABSTRACT: Utilization of the digital Landsat TM bands for automatic lineaments extraction and selection of the optimum bands are the main objects of this article. The classical method for lineament extraction was manually performed through aerial photographs and satellite imagery. Nowadays several commercial softwares are developed to deal with the automatic linear features extraction using the optical and radar data. In this research, GeoAnalyst PCI EASI/PACE software is used for lineaments extraction from Landsat TM data under the default parameters. Two case studies (East Gabal Nuqra and Gaziret Khashm Natash) represent different terrain categories have been investigated. Subsets covering these areas were obtained from the original Landsat TM imagery. Lineament is defined as straight or somewhat curved feature in the image. It is distinguished by sharp change in variance across its length as compared to the variance along it. The lineament extraction algorithm consists of three remarkable steps: edge detection, thresholding and linear extraction. Analyses of the results obtained in this study led to the coming conclusions:

- 1) Visible bands (1, 2 & 3) produced higher lineaments number (frequency) compared with SWIR bands (5 & 7). In the first study area, band-1 produced the highest lineaments number (1423) compared with band-5 (787) while in the second study area, band-2 scored the highest frequency (99) compared with band-7 (65).
- 2) The regional pattern of the extracted lineaments is characterized by a high degree of preferred orientation. The main trends of the extracted lineaments of band-1 in East Gabal Nuqra area are NW, NNE and N-S constituting 39.5%, 34.8% and 15% of the total number of lineaments. ENE, E-W and WNW are subordinate trends with 4.9%, 4.85% and 0.7% of the total number of lineaments, respectively. In Gaziret Khashm Natash area the main trends of the extracted lineaments of band-2 are NE, NNW, NW and NNE constituting 30.5%, 21%, 14.7% and 13.6% of the total number of lineaments. N-S and E-W are subordinate trends with 13.6% and 6.4% of the total number of lineaments, respectively.
- 3) In matching with the published data it revealed that the extracted lineaments are coinciding largely with the structural lines mapped by (Madani, 2000).
- 4) Careful inspection of panchromatic TM images of the study areas showed that the drainage lines are clearly observed in visible bands and faintly observed in SWIR bands. Most of these lines are structurally controlled and follow the main trends of the study areas.
- 5) Analysis of different structural elements in Gaziret Khashm Natash area revealed that the presence of a relationship between the lineament trends and the distribution of the ring dykes. In the author opinion the emplacement of the ring dykes is controlled by the intersection of the NE, NNE and NW trending faults.

1. INTRODUCTION

The concept of lineaments extraction from digital satellite images has been treated by several authors among them; (Podwysocki et al., 1975), (Burdick and Speirer, 1980) and (Baumgartner et al., 1999). Utilization of the digital Landsat TM bands for automatic lineaments extraction and selection of the optimum bands are the main tasks of this work. Two localities from Wadi Natash area, south Eastern Desert, Egypt (Fig. 1) are selected and investigated. They are namely "East Gabal Nuqra area" with an area about 22.5 Km ² 22.5 Km and "Gaziret Khashm Natash area" about 7.5 Km ² 5 Km. Subsets covering these test areas were obtained from the original Landsat TM imagery. A TM scene acquired by Landsat-5 has seven broad spectral bands. Six of these bands detect visible (1, 2 & 3), near infrared "NIR" (4) and short wave infrared "SWIR" (5 & 7) radiation (0.45um to 2.35um) and has a pixel size of about 30 ² 30 meters. The seventh band (6) detects thermal radiation with a resolution of 120 meters. The author used these bands for lineaments extraction using GeoAnalyst PCI EASI/PACE commercial software under the default parameters.

2. GEOLOGIC SETTING

Several authors studied the geology, petrography and geochemistry of the rock units exposed at Wadi Natash area, such as; (Barthaux, 1922), (Abou El-Gadayel, 1974), (Hubbard, 1981), (Hashad et al., 1982), (Hashad, 1994)

and (Madani, 2000). Four main different rock units are exposed at Wadi Natash area these are from oldest to youngest as follows:

- 1- Basement rocks (oldest).
- 2- Abu Agag Formation.
- 3- Wadi Natash volcanics.
- 4- Trachytic ring dykes (youngest).

Precambrian basement rocks represent the oldest rocks exposed at the area under consideration. They crop out near Gaziret Khashm Natash area and represented mainly by mafic to intermediate metavolcanics. They overlain unconformably by the Turonian sandstones of Abu Agag Formation. The volcanic rocks exposed at Wadi Natash area form a dissected plateau with pronounced stratified appearance. They occur in the form of sills, flows and ring dykes. The volcanic sequence consists of three distinct basal flows separated by two conglomeratic horizons (Hubbard, 1981). Four main volcanic flows (group I, group II, group III and group IV) separated by three erosional surfaces are recognized (Madani, 2000). These flows are extruded and cut by trachytic ring and semi-ring dykes.

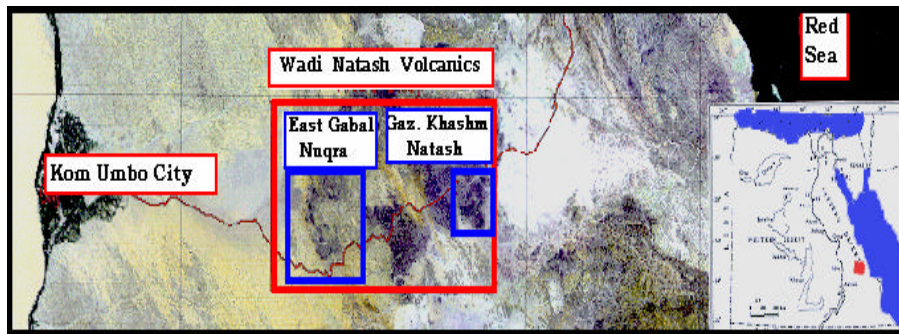


Figure 1: Location Map of The Study Area.

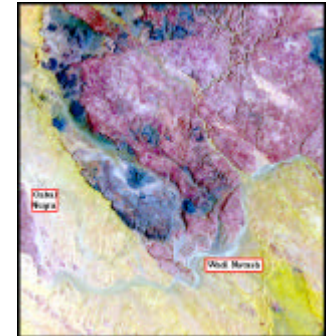


Figure 2: Landsat TM Color Composite Image, East Gabal Nuqra Area.

3. LINEAMENTS EXTRACTION, ANALYSES AND VALIDATION

The lineament extraction algorithm of GeoAnalyst PCI EASI/PACE software consists of edge detection, thresholding and linear extraction steps. These steps were carried out over VISIBLE, NIR and SWIR panchromatic images as well as band-6 under the default parameters of the software (Appendix “A”). In the following sections a detailed description of the analyses and results will be presented.

3.1 East Gabal Nuqra Area

East Gabal Nuqra area extends 7.5 Km eastward from Gabal Nuqra (Fig.2). It is covered by poorly sorted, immature sandstone representing the Turonian Abu Agag Formation with extrusion of black olivine basalt. They are easily discriminated on the basis of Landsat color composite image bands 7(red), 4(green) and 1(blue) in which sandstone and olivine basalt have brick-red and deep blue image signatures respectively.

The obtained fracture pattern is shown in Figures 3 & 4 respectively. Furthermore, Figure 3 demonstrates the automatically extracted lineaments over the six VISIBLE, NIR and SWIR bands. Figure 4, shows the automatically extracted lineaments over the thermal band (band-6).

The relationship between the automatically extracted lineaments number (frequency) and Landsat TM bands is shown in Table 1. It has been noticed that the visible bands have higher lineaments number compared with short wave infrared “SWIR” bands. The highest score of the lineaments number is recorded in the visible bands and arranged as follows: band-1 (1423), band-2 (1264) and band-3 (1060) whereas the lowest score of the lineament number is recorded in SWIR bands (band-5 “787” and band-7 “887”). The regional pattern of the extracted lineaments is characterized by strong degree of preferred orientation.

Table 1: Landsat TM Bands Versus Lineaments Frequency, East Gabal Nuqra Area.

TM Bands	Lineaments # (Frequency)
Band-1 (Visible-Blue 0.45 – 0.52 um)	1423
Band-2 (Visible- Green 0.52-0.60 um)	1264
Band-3 (Visible- Red 0.63 – 0.69 um)	1060
Band-4 (Near Infra Red 0.79-0.90 um)	1071
Band-5 (Short Wave Infra Red 1.55 – 1.75 um)	787
Band-6 (Thermal)	887
Band-7 (Short Wave Infra Red 2.08 – 2.35 um)	887

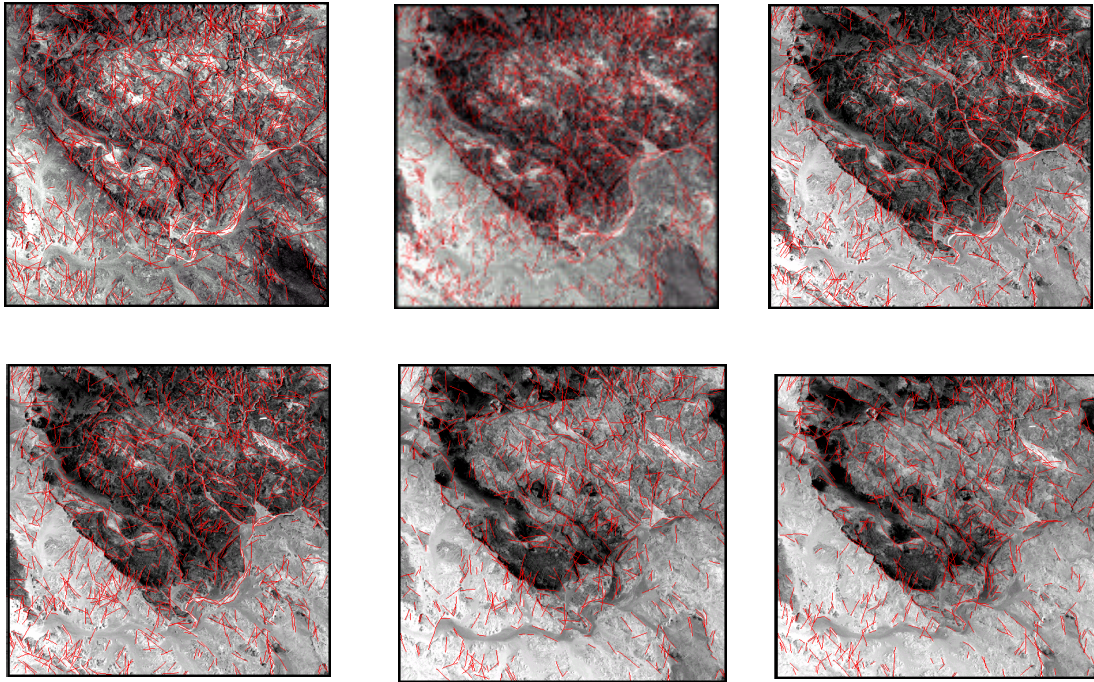


Figure 3: Automatic Extracted Lineaments Over The Six VISIBLE, NIR And SWIR Bands, East Gabal Nuqra.

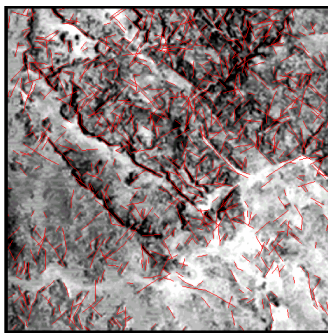


Figure 4: Automatic Extracted Lineaments Over Band-6.

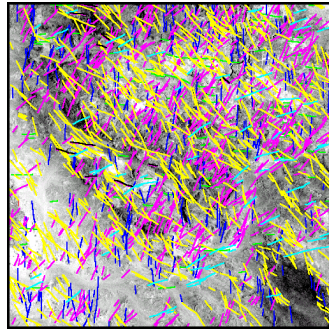


Figure 5: Main Lineament Trends Extracted From Band-1.

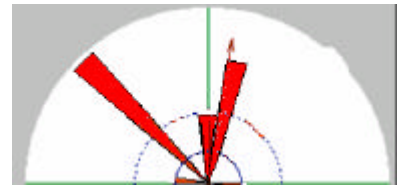


Figure 6: Lineaments Frequency Rose Diagram.

Figure 5, depicts the main trends of the lineaments extracted from band-1. A total of 1423 lineaments were automatically extracted. The main trends are NW, NNE and N-S constituting 39.5%, 34.8% and 15% of the total number of lineaments. ENE, EW and WNW are subordinate trends with 4.9%, 4.85% and 0.7% of the total number of lineaments, respectively. The relationship between the main trends and lineaments frequency is shown in Table 2. Figure 6, represents the lineaments frequency rose diagram. It shows the high degree of preferred orientation particularly in NW, NNE and N-S trends. In matching with the previous works carried out in this area, three main structural lines were traced by (Madani, 2000). The first is a master ENE dextral-slip fault traversing the Turonian Abu-Agag Formation. The other two trends (NW and NE) are extensional faults and affected both sandstone and overlying younger basalts.

Table 2: The Main Lineament Trends And Their Frequency Over Band-1, East Gabal Nuqra Area.

Main Directions	Frequency	Frequency %
NW	561	39.5%
NNE	496	34.8%
N-S	217	15.3%
ENE	70	4.9%
E-W	69	4.8%
WNW	10	0.7%

3.2 Gaziret Khaskm Natash Area

Gaziret Khaskm Natash area lies at the mouth of Wadi Natash and is represented by trachytic ring dyke. Basalt, hawaite, mugearite, benmorite and trachyte are the main rock units exposed in this area. From the Landsat color composite image bands 7(red), 4(green) &1(blue) (Fig.7), it is easy to discriminate between the previous mentioned rock units where they have green, red and cyan colors.

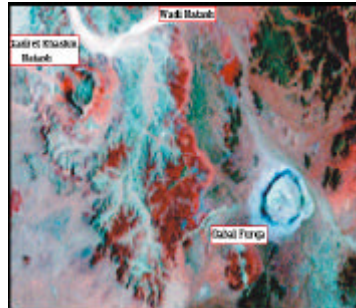


Figure 7: Landsat TM Color Composite Image, Gaziret Khaskm Natash Area.

The automatically extracted lineaments obtained are presented in Figures 8 &9 respectively. The extracted lineaments over VISIBLE, NIR and SWIR bands are shown in Figure 8 while Figure 9, demonstrate the extracted lineaments over the thermal band (band-6). Band-6 is excluded from the comparison due to its lower spatial resolution (120 meters).

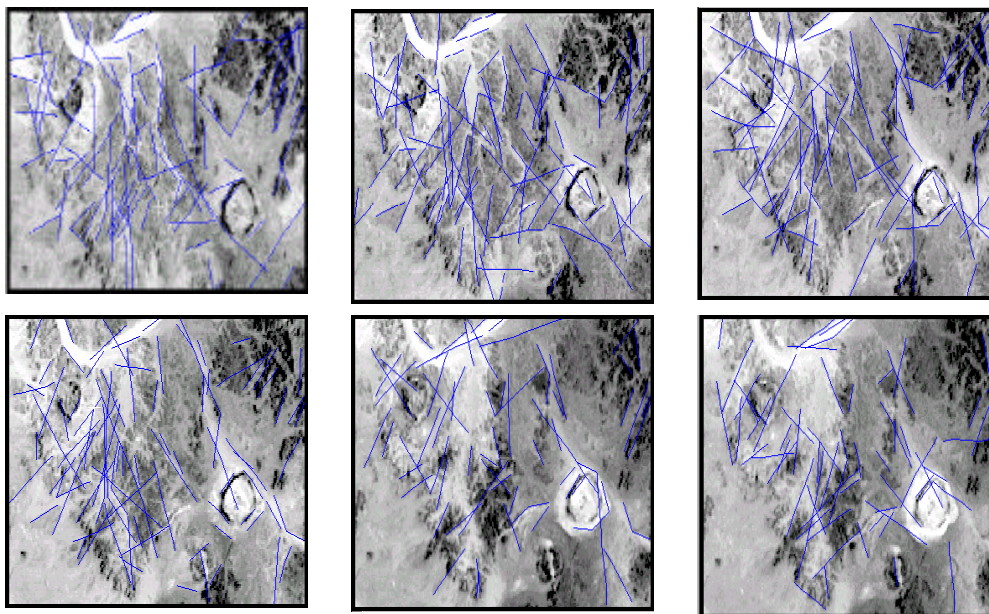


Figure 8: Automatic Extracted Lineaments Over Six VISIBLE, NIR And SWIR Bands, Gaziret Khaskm Natash.

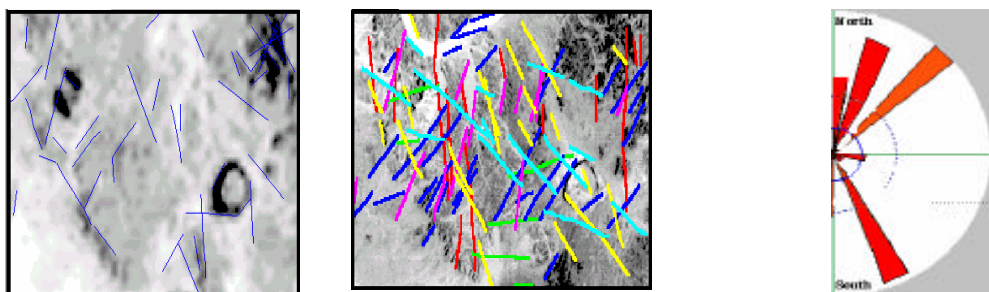


Figure 9: Automatic Extracted Lineaments Over Band-6.

Figure 10: Main Lineament Trends Extracted From Band-1.

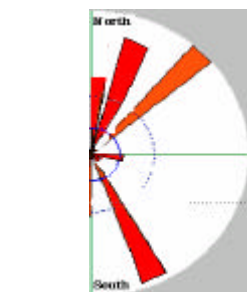


Figure 11: Lineaments Frequency Rose Diagram.

Table 3, shows the lineaments frequency over Landsat TM seven bands. It is worth mentioning that the visible bands have higher lineaments number compared with short wave infrared “SWIR” bands. The highest score

of the lineaments number is recorded in the visible bands and arranged as follows: band-2 (99), band-3 (95) and band-1 (94) whereas the lowest score of the lineament number is recorded in SWIR bands (band-5 “69” and band-7 “65”). The extracted lineaments are characterized by strong degree of preferred orientation and behave the following directions: NW, WNW, NE, NNE, NS and E-W.

Table 3: Landsat TM Bands Versus Lineaments Frequency, Gaziret Khashm Natash Area.

TM Bands	Lineaments # (Frequency)
Band-1 (Visible-Blue 0.45 – 0.52 um)	94
Band-2 (Visible- Green 0.52-0.60 um)	99
Band-3 (Visible- Red 0.63 – 0.69 um)	95
Band-4 (Near Infra Red 0.79-0.90 um)	92
Band-5 (Short Wave Infra Red 1.55 – 1.75 um)	69
Band-6 (Thermal)	43
Band-7 (Short Wave Infra Red 2.08 – 2.35 um)	65

Figure 10, shows the main lineament trends extracted from band-2. A total of 99 lineaments were automatically extracted. The main trends are NE, NNW, NW and NNE constituting 30.5%, 21%,14.7% and 13.6 of total number of all lineaments. NS and E-W trends are subordinate with 13.6% and 6.3% of total lineament number. Table 4, shows the relationship between the main trends and lineaments frequency. Figure 11, represents the lineaments frequency rose diagram. The pattern shows the presence of high degree of preferred orientation particularly in NE, NNW, NW and NNE trends. Madani (2000) recognized two main extensional faults in this area (NW and NE). He added that the NW faults are extending for long distances parallel to the Mesozoic Kom-Umbo-Nuqra-Kharit rift basin.

Table 4: The Main Lineament Trends And Their Frequency Over Band-2, Gaziret Khashm Natash Area.

Main Directions	Frequency	Frequency %
NE	29	30.5%
NNW	20	21%
NW	14	14.7%
NNE	13	13.6%
N-S	13	13.6%
E-W	6	6.3%

4. RING DYKES AND THE EXTRACTED LINEAMENTS

One of the most fascinating features in Gaziret Khashm Natash area is the presence of the ring dykes. It can be easily distinguished on the Landsat imagery by their circular (Gabal Furqa) to semi-circular (Gaziret Khashm Natash) shape (Fig. 7). Several authors studied the field occurrence and geochemistry of the ring dykes distributed at Wadi Natash area. (El-Ramly et al., 1970) stated that the tectonic distribution of ring complexes is controlled by NW and NE trends. (Garson and Krs, 1976) identified a large-scale shear zone and deep-seated tectonic fractures trending N30W and N60E. (Madani, 2000) mentioned that vulcanicity of Wadi Natash area began through NW trending fissures parallel to Kom-Umbo rift system dated to the Cretaceous time. Figure 12, shows the distribution of ring dykes in Gaziret Khashm Natash area in relation to the main lineament trends extracted in this work. The presence of these ring dykes indicates the more extensional stresses received in this area. The ring dykes are located at the intersection of the NE and NW trending faults. Gabal Furqa and Gaziret Khashm Natash ring dykes were extruded through the intersection of NE and NW trending faults. These faults formed as a result of different stresses affected the area during the Late Cretaceous time. The present author believes that the source of these stresses is attributed to mantle upwelling, which cause crustal collapse before the extrusion of trachytic melt.

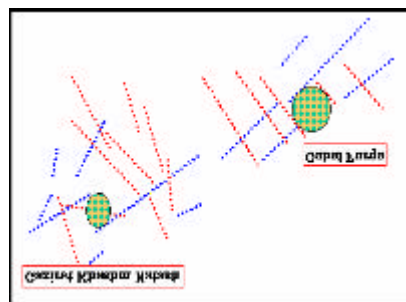


Figure 12: The Main Lineaments Trends Versus The Ring Dykes, Gaziret Khashm Natash.

5. DISCUSSION AND CONCLUSIONS

Based on visual photo interpretation, it can be deduced that the SWIR bands (5&7) have high degree of lithologic discrimination compared with the visible bands (1,2&3). This could be attributed to the atmospheric scattering effect. The atmospheric scattering is high in shorter wavelength regions compared with longer wavelengths. The author expected that the high lineaments number extracted by the GeoAnalyst software would be obtained in SWIR bands rather than in visible bands. But the results are completely incompatible with what was expected. The visible bands scored the highest lineaments frequency whereas the SWIR bands scored the lowest. Careful inspection of Landsat TM images demonstrates that the drainage lines (network) are clearly observed in visible bands and they are faintly observed in SWIR bands (Figs. 14a&b). The drainage lines are considered as lineaments according to the lineament definition. From the foregoing data, it could be concluded:

- 1) Short wave infrared bands have the higher lithologic discrimination compared with the visible bands.
- 2) Visible bands are the optimum bands for automatic lineaments extraction compared with SWIR bands in the areas covered by sandstone extruded by volcanic rocks and under the default parameters of GeoAnalyst PCI EASI/PACE software.
- 3) The most important feature in Gaziret Khashm Natash area is the presence of ring dykes. It is clearly to issue that, there is good relationship between the lineament trends and the distribution of the ring dykes. The author believed that the emplacement of the ring dykes is controlled by the intersection of the prevailing NE, NNE and NW trending faults.

ACKNOWLEDGEMENTS

The author is indebted to GeoMAP Consultants members for their fruitful discussions. Cordial thanks are due to Prof. Dr. M. El-Sharkawy, Dr. M. Abdel Wahed and Dr. M. Mansour, Geology Department, Faculty of Science, Cairo University for their kindly reviewing the manuscript.

REFERENCES

- Abou El-Gadayel, A., 1974. Contribution to the geology and geochemistry of Wadi Natash lava flows, M.Sc. thesis, Cairo Univ., Egypt.
- Barthoux, J.C., 1922. Chronologie et description des roches ignees du Desert Arabique. Mem. Inst. Egypte. Le Caire.
- Baumgartner, A., Steger, C., Mayer, H., Eckstein, W. and Ebner, H., 1999. Automatic road extraction based on multi-scale, grouping and context. Photogrammetric Engineering and Remote Sensing, (65), pp. 777-785.
- Burdick, R. G., and Speirer, R. A., 1980. Development of a method to detect geologic faults and other linear features from Landsat images. U. S. Bureau of Mines Report Inv., 8413:74.
- El-Ramly, M.F., Budanov, V.L., Hussein, A., A. and Derenluk, N.E., 1970. Ring Complexes of the South-Eastern Desert of Egypt. Geol. Surv. Egypt. pp. 181-194.
- Garson, M., S. and Krs, M., 1976. Geophysical and geological evidences of the relationship of Red Sea transverse tectonics to ancient features. Geol. Soc. Am. Bull. (87), pp. 69-181.
- Hashad, A.H., Hassan, M.A. and Aboul Gadayel, A.A., 1982. Geological and petrological study of Wadi Natash Late Cretaceous volcanics. Egypt. J. Geol., (26)1, pp.19-37.
- Hashad, M.H., 1994. geochemical characteristics and petrogenesis of Phonolitic trachytic plugs associated with Wadi Natash volcanic rocks. M.E.R.C. Ain Shams Univ., Earth Sci. Ser., (8), pp.131-145.
- Hubbard, H.B., 1981. Geochemical evolution of the Wadi Natash volcanic field, an alkaline basalt flood in the Eastern Desert of Egypt. M.Sc. Thesis, Univ. South Carolina, U.S.A.
- Madani, A. A., 2000. Geological studies and remote sensing applications on Wadi Natash volcanics, Eastern Desert, Egypt. Ph.D. Thesis, Faculty of Science, Cairo University.
- Podwysocki, M. H., Moik, J. G., and Shoup, W. D., 1975. Quantification of Geologic Lineaments by Manual and Machine Processing Techniques. Proc. NASA Earth Resources Survey Symposium, Houston, Texas, pp. 885-903.

Appendix "A"

Default Parameters of GeoAnalyst PCI EASI/PACE Software:

- | | |
|--|--|
| -Edge filter radius (1..1024) = 3 | -Minimum edge gradient (0..255) = 15 |
| -Minimum line length (1..1024) = 15 | -Line fitting tolerance (1..10) pixels = 2 |
| -Maximum angular difference (0..90) degrees = 10 | -Maximum linking distance (0..1024) = 30 |